International Journal of Recent Engineering Research and Development (IJRERD)
ISSN: 2455-8761
www.ijrerd.com || Volume 05 – Issue 11 || November 2020 || PP. 09-13

Numerical Study of flow field Conventional and Elliptical Blade of the Savonius Wind Turbines

Arifin Sanusi[1]
[1]Department of Mechanical Engineering, Nusa Cendana University,
Jalan Adi Sucipto, Kupang, 85001, Indonesia

Abstract: Fluid flow is very helpful in analyzing the flow phenomenon described in numerical simulations that occur around the blades in the rotor of a turbine. This paper aims to numerically analyze the flow patterns around the blades of a Savonius wind turbine using Ansys_Fluent 14.5. computational fluid dynamics (CFD). The flow is depicted in the form of a contour of static pressure and velocity that occurs around the blade. To show the difference in flow around the blade, conventional and elliptical blade rotor models were simulated. The simulation and analysis results show that there is a very significant effect on the flow that occurs and affects the performance of the Savonius wind turbine.
Keywords: fluid flow, CFD, wind turbine, blade rotors

1 Introduction

The Savonius wind turbine is one type of vertical shaft wind turbine that is still being developed to increase its efficiency, because according to Zhou and Rempfer, 2013[1] is still low compared to other types of turbines. The construction of the Savonius wind turbine is quite simple and can receive wind from all directions, so it is suitable to be developed by the community because it can use materials that are widely marketed and do not require high poles. Visualization through simulation can show the flow pattern that occurs so that analysis can be carried out to see what causes the thrust and what causes obstacles. According to Nakajima, 2008[2] there were six influential flow patterns around the turbine rotor. The flow model in the form of vortex separation and stagnation points is a phenomenon in fluid flow that can reduce the performance of the turbine. The attached flow pattern produces thrust and lift, while the flow model in the form of dragging flow produces power on the convex side of the forward blade and jet flow in the blade gap (overlap flow) produces pressure on the concave side of the blade back, so that will affect the performance of the rotor, thus the flow pattern contributes to an increase in the coefficient of power and torque in the turbine. The separation of the vortex at the forward blade tip and the blade end from the returning blade, as well as the separation of the vortex that grows as the flow downstream of the rotor, will affect reducing rotor performance[2].

Based on a particular flow configuration, different geometries give different results. To improve the performance of these turbines, researchers have carried out research and modification of the Savonius turbine rotor construction using different methods both experimentally and numerically.The performance of the Savonius turbine rotor is influenced by flow parameters and turbine geometry[3]. The Savonius turbine turbines with conventional and elliptical blades provide different shapes. The source of the difference is the significant laminar part of the boundary layer[4].Therefore this research is analyzed numerically around the propeller of a Savonius wind turbine using computational fluid dynamics (CFD) on conventional and elliptical blades.

2 Numerical Simulation

2.1 Design Rotor Blade

The blade shape used for the simulation consists of an elliptical blade and a conventional blade according to the research results of Kacprzak et al., 2013[4] (Fig.1). As for the simulated savonius turbine blade shape, it is made in a modular design according to the size as in the following figure; Conventional blade model was semicircular with a radius of R = 57.5 mm, and the Elliptical blade was a curved line connecting the coordinate points A (15 mm; 0), B (-50 mm; 50 mm), C (-100 mm; 0), where the line connecting points A and B were spline and connecting points B and C were the lines of a quarter circle with a radius of R1 = 50 mm.

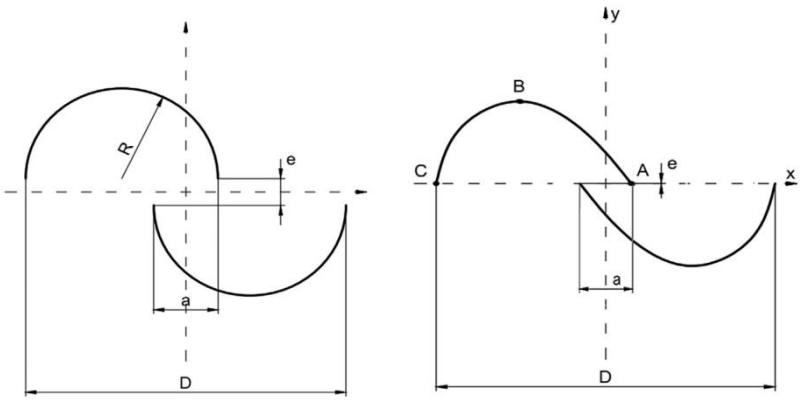

(a) Conventional blade (b) Elliptical balde

Figure 1: Blade rotors Savonius[4]

2.2 Scheme simulation

The program simulation procedure is carried out by identifying the dimensions of the turbine by making a blade model using Ansys-Design Modeler 14.5, as well as creating a mesh and boundary conditions and fluid properties with CFD-Fluent to be used in the computational domain. After that, it is continued by simulating the airflow as input to the turbine rotor with a wall that is considered to be non-slip and the airflow out as an output, as in the following simulation domain scheme.

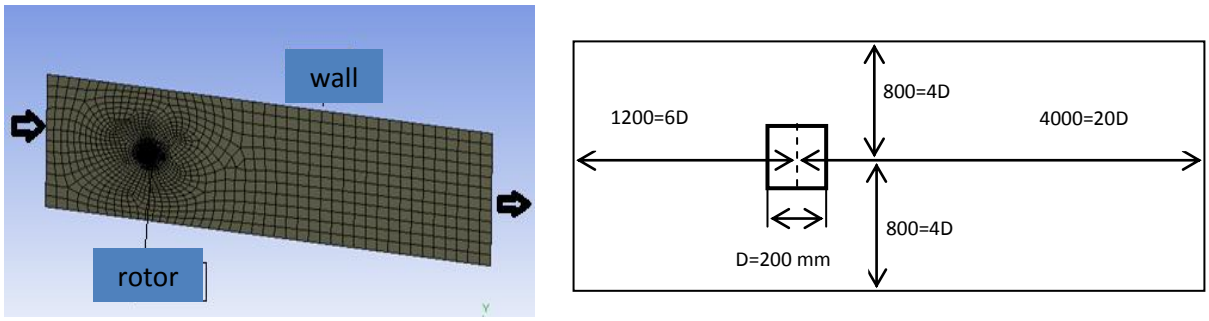

Figure 2: Simulation domains

General steps for implementing the numerical method are as follows:

- Identification of problems
- Pree processor, at this stage, consists of:
  - geometry creation using Ansys Fluent 14.5 Design Modeler software for all blade models.
  - the meshing process is carried out by sliding mesh by testing mesh-1 of around 40,000; mesh-2 80,000 and mesh-3 120,000, followed by grid testing to select a sufficiently accurate mesh count in subsequent analyzes.

The meshing process is in the form of a rectangle for the two-blade models in Figure 3. The number of meshes with the volume up to the fluid differs according to the shape of the blade using automatic meshing in the following table:

Table 1: The number of mesh in each fluid and theblade rotors

Blade rotors	Elliptical	Conventional
fluid	47.556	81.859
rotor	2.914	1.676
All Domains	50.470	83.535

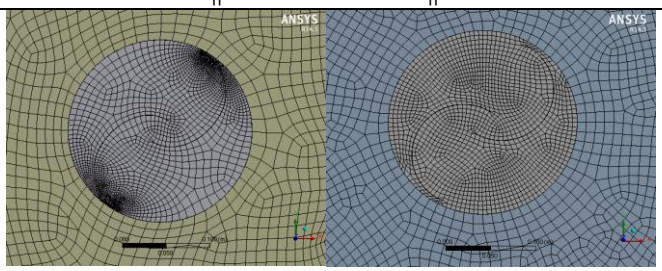

(a) **(b)**

Figure 3: Mesh rotor(a) elliptical blade,(b) conventional blade

The analysis focused on the effects in the area of rotor testing with two-dimensional simulation. The conservative or divergence form of the system of equations which governs the time-dependent two-dimensional fluid flow of an incompressible Newtonian fluid. The following differential form of the governing equation is provided according to the computational model and their corresponding approximation as follows:

the conservation of mass equation or continuity equation is given by

$$\frac{\partial \rho}{\partial t} + \frac{\partial (\rho u)}{\partial x} + \frac{\partial (\rho v)}{\partial y} = 0 \quad (1)$$

the conservation of momentum equation is given by

Momentum – x

$$\rho \frac{Du}{Dt} = \frac{\partial (-p+\tau_{xx})}{\partial x} + \frac{\partial \tau_{yx}}{\partial y} + S_{Mx} \quad (2)$$

Momentum – y

$$\rho \frac{Dv}{Dt} = \frac{\partial \tau_{xy}}{\partial x} + \frac{\partial (-p+\tau_{yy})}{\partial y} + S_{My} \quad (3)$$

The k-ε realizable model is substantially better than the standard k-ε model for many applications [1]. So that in this simulation, the transport equation for the k-ε realizable model was used as follows:

$$\frac{\partial (\rho k)}{\partial t} + \frac{\partial (\rho k \mu_i)}{\partial x_i} = \frac{\partial \left[\left(\mu + \frac{\mu_t}{\sigma_k} \right) \left(\frac{\partial k}{\partial x_j} \right) \right]}{\partial x_j} + P_k + P_b - \rho \varepsilon - Y_M + S_k \quad (4)$$

$$\frac{\partial (\rho \varepsilon)}{\partial t} + \frac{\partial (\rho \epsilon \mu_i)}{\partial x_i} = \frac{\partial \left[\left(\mu + \frac{\mu_t}{\sigma_\epsilon} \right) \left(\frac{\partial \epsilon}{\partial x_j} \right) \right]}{\partial x_j} + \rho C_1 S_\epsilon - \rho C_2 \frac{\epsilon^2}{k + \sqrt{\nu \epsilon}} + C_{1\epsilon} \frac{\epsilon}{k} C_{3\epsilon} G_b + S_\epsilon \quad (5)$$

The turbulence viscosity was determined by $\mu_t = \rho C_\mu \frac{k^2}{\varepsilon}$ (6)

The downstream pressure on the output 1 atm absolute, the density of the fluid ρ = 1.225 kg/m^3, the fluid dynamic viscosity μ = 1.7895 x105 N.s/m^2. The variations of air density were ignored and not treated as incompressible using asymmetric flow, so that the flow of vertical may be neglected. The criterion for convergence in the analysis of flow is 10^{-3} and 30 iterations per time step. The simulation is carried out for 30000-time steps to have many complete rotations.

3 Results and Discussion

The flow pattern that occurs around the rotor blade is very important information and is needed in numerical analysis. The simulation results using Ansys_Fluent Release 14.5 software, show the flow pattern in contourvelocity of the elliptical blade (Fig. 4a) and the conventional blade (Fig.4b) showing different flow patterns.

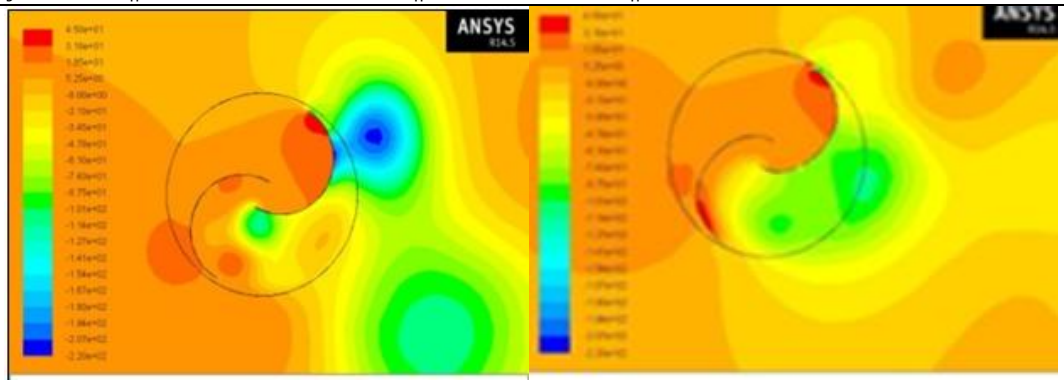

(a) **(b)**

Figure 4: Contour static pressure a) conventional blade, b) elliptical blade

Figure 4, shows the static pressure distribution that occurs in the rotor with a conventional blade and an elliptical blade. The pressure on the concave side of the blade is the main source in producing turbine performance. Static pressure is very influential onthe static torque. The starting star capability of vertical axle turbines is determined by the static torque performance[5]. The pressure on the concave side of the pressure bar that occurs on the convex side advances the blade and there is an overlap of the rotor blades. The increased pressure on the concave side which returns the blades to contribute increases the positive torque in the turbine[6]. The convex side pressure of the conventional blade shows a low pressure on both the outer ends of the blade forward and the convex side returns a fairly large stagnation point [Fig. 4a]. The elliptical blade occurs with low pressure on the convex side that moves the blade forward and tends to expand towards the inner end of the blade, but the stagnation point on the convex side returns the smaller blade [Fig. 4b]. The low-pressure contribution on the convex side of the blade advances a large role in improving the performance of the turbine[1]. However, it is seen that the conventional blade tends to make a vortex, thus inhibiting and reducing the performance of the rotor blade. The static pressure model on the convex side pushing the blade affects the pressure on the back of the blade. The stagnation point that occurs on the convex side returning blade to appear different according to the low-pressure difference on the convex side of the blade.

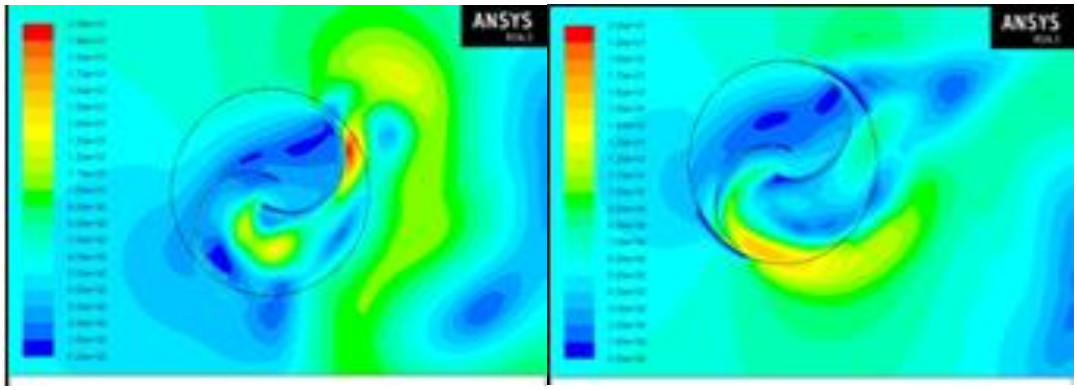

(a) **(b)**

Figure 4: Contour velocitya) conventional blade, b) elliptical blade

Figure 5 shows the contour velocity of the different rotor blades. There is a clear difference in fluid flow between the conventional blade and the elliptical blade, especially the flow around the overlap. This phenomenon is inseparable from the influence of the overlap jet, which provides flow to compress the concave side of the returning blade and results in a positive torque increase in the turbine rotor. At the outer end of the advancing blade, you can see that the recirculation flow is quite prominent on the conventional blade compared to the elliptical blade. The recirculating flow results in decreased performance of the turbine rotor and vortices on the convex side of the advancing blade that rotates clockwise, increasing the suction pressure strength and causing a decrease in torque[1]. Based on this, the fluid flow behind the rotor blade greatly affects the performance of the turbine, including the shear force that occurs. The results of the visualization of the flow through the Savonius rotor identified six main flow patterns that occur in the rotor blades that affect the operational characteristics of the turbine. Three types of flow contribute to improved performance, namely:

attached flow, dragging flow, and overlap flow, while flow affects decreasing the performance of each; stagnation flow, vortex flow of advancing and returning blade[2]. Flow from the convex side of the advancing blade and flow from the overlap creates a vortex at the inner end of the advancing blade (Fig. 5). The conventional blade (Fig. 5a) has a larger vortex near the blade tip, whereas the elliptical blade is seen expanding outward from the rotor. The near-overlap flow structure is very complex and is influenced by stagnation flow along the concave side of the advancing blade, and the Coanda-like flow along the concave side of the returning blade, and the presence of circulating flow in the center of the rotor[7]. The Coanda-like flow as vorticity flow in the overlap area of the Savonius turbine which migrates from the tip side of the advancing blade to the concave side of the returning blade[6]

4 Conclusions

In the simulation results and analysis of counter pressure and counter velocity, it is neglected that the development of the Savonius turbine rotor model with an elliptical blade causes changes in fluid flow compared to using a semi-circular conventional blade, The same overlap dimensions, the elliptical blade provides greater jet flow and generates thrust on the recessed side of the blade back and reduces recirculation flow that occurs on the convex side of the forward blade thereby increasing positive torque compared to conventional blades.

References

[1]. T. Zhou and D. Rempfer, "Numerical study of detailed flow field and performance of Savonius wind turbines," *Renew. Energy*, vol. 51, pp. 373–381, Mar. 2013, doi: 10.1016/j.renene.2012.09.046.

[2]. M. Nakajima, I. I. O. Shouichiro, and T. Ikeda, "Performance of Savonius rotor for environmentally friendly hydraulic turbine," *J. Fluid Sci. Technol.*, vol. 3, no. 3, pp. 420–429, 2008.

[3]. J. V. Akwa, H. A. Vielmo, and A. P. Petry, "A review on the performance of Savonius wind turbines," *Renew. Sustain. Energy Rev.*, vol. 16, no. 5, pp. 3054–3064, Jun. 2012, doi: 10.1016/j.rser.2012.02.056.

[4]. K. Kacprzak, G. Liskiewicz, and K. Sobczak, "Numerical investigation of conventional and modified Savonius wind turbines," *Renew. Energy*, vol. 60, pp. 578–585, Dec. 2013, doi: 10.1016/j.renene.2013.06.009.

[5]. S. Roy and U. K. Saha, "Computational Study to Assess the Influence of Overlap Ratio on Static Torque Characteristics of a Vertical Axis Wind Turbine," *Procedia Eng.*, vol. 51, pp. 694–702, 2013, doi: 10.1016/j.proeng.2013.01.099.

[6]. N. Fujisawa, "On the torque mechanism of Savonius rotors," *J. Wind Eng. Ind. Aerodyn.*, vol. 40, no. 3, pp. 277–292, 1992.

[7]. N. Fujisawa, "Velocity measurements and numerical calculations of flow fields in and around Savonius rotors," *J. Wind Eng. Ind. Aerodyn.*, vol. 59, no. 1, pp. 39–50, 1996.